



Neuroradiology/Head and Neck Imaging Original Research

Diffuse Infiltrative Non-mass-like Brain Parenchymal Lesions on MRI: Differentiating Lymphomatosis Cerebri from its Mimics

Anurima Patra¹, Anitha Jasper¹, Harshad Vanjare¹, Geetha Chacko², Sherin Susheel², Ajith Sivadasan³, Julie Hephzibah⁴, Pavithra Mannam¹

Departments of ¹Radiology, ²Pathology, ³Surgery and ⁴Nuclear Medicine, Christian Medical College and Hospital, Vellore, Tamil Nadu, India.



***Corresponding author:**

Pavithra Mannam,
Department of Radiology,
Christian Medical College and
Hospital, Vellore, Tamil Nadu,
India.

pavithra.mannam@gmail.com

Received : 11 April 2021

Accepted : 25 June 2021

Published : 23 July 2021

DOI

10.25259/JCIS_75_2021

Quick Response Code:



ABSTRACT

Objectives: Diffuse infiltrative “non-mass-like” parenchymal lesions on MRI brain are a known presentation of an aggressive condition called lymphomatosis cerebri (LC) but are often misdiagnosed due to its non-specific clinical and imaging findings. We aim to identify clues to differentiate lymphomatosis from its less aggressive mimics based on imaging features.

Material and Methods: MRI brain studies showing diffuse infiltrative “non-mass-like” parenchymal lesions between January 2013 and March 2020 were retrospectively identified and read for lesion location, signal characteristics, and enhancement pattern by two radiologists. Additional findings on MRI spine and whole-body fluorodeoxyglucose (FDG) positron emission tomography-computed tomography (PET-CT) were recorded wherever available. The clinical diagnosis, patient demographics, symptoms, laboratory and histopathology results, treatment details, and follow-up details were also noted.

Results: Of the 67 patients, 28 (41.7%) were diagnosed with lymphomatosis. The remaining 39 (13.4%) patients were classified as non-lymphomas (infective, vasculitis, and inflammatory conditions). Diffusion restriction on MRI (20/67, $P = 0.007$) and increased regional activity on FDG PET-CT (12/31, $P = 0.017$) were the two imaging parameters found to significantly favor lymphomatosis over other conditions, whereas the presence of microhemorrhages on susceptibility-weighted imaging was significantly associated with vasculitis ($P = 0.002$). Rapid clinical or imaging deterioration on a short trial of steroids ($P = 0.00$) was the only relevant clinical factor to raise an early alarm of lymphomatosis. Positive serological markers and non-central nervous system systemic diseases were associated with non-lymphomatous diseases.

Conclusion: LC and its less aggressive mimics can be differentiated on diffusion-weighted imaging-MRI and PET-CT when read in conjunction with rapid progression of clinical features, serological workup, and systemic evaluation.

Keywords: Lymphomatosis, Vasculitis, Demyelination, Infiltrative brain lesions

INTRODUCTION

Diffuse infiltrative “non-mass-like” parenchymal lesions on MRI brain have a long list of differentials such as demyelination, immune-mediated disorders vasculitis, progressive multifocal leukoencephalopathy (PML), and encephalitis.^[1] Although less common, lymphomatosis cerebri (LC) can present in a similar fashion.^[2,3] It is a rare and diffusely infiltrative variant of primary

This is an open-access article distributed under the terms of the Creative Commons Attribution-Non Commercial-Share Alike 4.0 License, which allows others to remix, tweak, and build upon the work non-commercially, as long as the author is credited and the new creations are licensed under the identical terms.

©2021 Published by Scientific Scholar on behalf of Journal of Clinical Imaging Science

central nervous system (CNS) lymphoma, and most sinister in the spectrum of “non-mass-like” brain lesions. Patients present in the age group of 50–70 years with non-specific clinical features ranging from gradual personality changes to rapid cognitive decline or neurological deficits.

The MRI features of LC are described as diffuse, infiltrative T2W hyperintense non-enhancing lesions that can involve any part of the CNS including supratentorial or infratentorial structures, cerebral white matter, or deep gray nuclei in unilateral or bilateral distribution, and the spinal cord. These findings are very different from the CNS lymphomas that typically present as T2W hyperintense and nodular contrast-enhancing mass lesions. Due to the non-specific clinical and radiological findings, brain biopsy is recommended to yield a definitive diagnosis of LC. However, biopsy is often performed when patients are non-responsive to empirical immunomodulation therapy, which may result in considerable delay in diagnosis. Long-term steroids can also mask the clinical and imaging features of LC leading to disease progression and poor prognosis.^[2,4]

Differentiation of LC purely based on imaging is a challenge for radiologists due to the imaging similarities this condition shares with the benign counterparts, such as the absence of discrete mass formation, absent or patchy post-contrast enhancement, and variable diffusion restriction.^[2] These lesions are often initially judged to belong to the inflammatory or demyelinating spectrum, especially in the setting of a negative laboratory workup. These benign entities are more commonly encountered in clinical practice and often require observation to confirm the diagnosis. This further contributes to the delayed diagnosis of LC.

We aim to study the patterns of these “non-mass-like” infiltrative lesions on MRI brain and identify clues to differentiate LC from its mimics. We also aim to study the value of fluorodeoxyglucose (FDG) positron emission tomography-computed tomography (PET-CT) and laboratory investigations to aid in its diagnosis.

MATERIAL AND METHODS

Patient selection

We conducted an institutional review board approved (IRB no. 11221/2020) retrospective study on patients who underwent MRI brain in a tertiary care teaching hospital. Baseline MRI brain studies performed at a single institute, between January 2013 and March 2020, were searched from PACS for keywords of “inflammatory,” “immune mediated,” and “atypical lymphoma” in the reports. The images of 100 MRIs identified from the search were reviewed for the presence of “ill-defined diffusely infiltrative long TR (>5000 ms) hyperintense lesions without mass-like configuration or mass-like enhancement” by two radiologists. After excluding

33 cases that did not meet our primary study criteria, 67 patients were selected for the study. The exclusion criteria were (i) absence of baseline pre-treatment MRI at the same institute, (ii) absence of T2W or diffusion-weighted imaging (DWI) or post-contrast imaging, (iii) mass-like configuration with well-demarcated borders on MRI, (iv) patients receiving steroids or immunomodulators elsewhere before presenting at our institute, and (vii) absence of clinical or imaging follow-up within 6 months of presentation. Cases with degenerative or small vessel ischemic changes presenting as non-mass signal changes in deep white matter were also excluded from the study.

In the selected group of 67 cases, all the MRI brain images were reviewed by one neuroradiologist with 6 years of experience. In addition, findings on MRI spine and whole-body PET-CT were documented wherever available. Electronic medical charts were reviewed for clinical presentation and relevant laboratory data including cerebrospinal fluid (CSF) and histopathology results. Treatment details and follow-up imaging findings were also noted.

Reference standard

The patients were classified into two broad clinical diagnoses: lymphoma and non-lymphoma. The patient characteristics and final diagnoses are summarized in Table 1. Histopathology results were used as the reference standard for the patients who underwent a stereotactic brain biopsy. For the cases that did not undergo biopsy, the consensus clinical diagnosis available in the electronic medical records was considered the reference standard. This took into consideration the documented discussion of clinical findings, laboratory investigations, systemic manifestations, imaging findings, and treatment response in the multidisciplinary team meetings.

MRI protocol

MRI was performed following the standard institutional protocol on a 1.5 T (Siemens Healthcare, Erlangen, Germany) or 3 T (Philips Healthcare, Netherlands) unit. The sequences reviewed were as follows: Axial T2W FSE (TR = 5000 ms, TE = 95 ms), T1W (TR = 1900 ms, TE = 3 ms), axial FLAIR (TR = 9000 ms, TE = 90 ms, TI = 2200 ms), axial DWI (b=1000, TR = 4100 ms, TE = 90 ms), susceptibility-weighted imaging (SWI), and post-contrast images in all three planes after intravenous (i.v.) administration of gadopentetate dimeglumine at a dose of 0.1 mmol/kg body weight.

Image interpretation

The brain parenchymal lesions were categorized based on their location (supratentorial, infratentorial, or

Table 1: Summary of patient demographics, etiologies, CSF, and PET-CT results.

Characteristics	Number of patients (n=67)
Median age in years (range)	37 (18–72)
Sex	
Men	42
Women	25
Median weeks from baseline MRI to follow-up (range)	19 (4–23)
Biopsy diagnosis available	28 (41.7%)
Lymphoma	20
Gliosis	3
Inflammatory	4
Aspergillosis	1
Etiology	
Lymphoma	28 (41.7%)
Biopsy proven	20
Others	8
Infections	10 (14.9%)
Tuberculosis	6
Meliodosis	1
Toxoplasmosis	2
Aspergillosis	1
Inflammatory	22 (32%)
Immune mediated	12
Behcet disease	1
Encephalitis	2
PML	2
Lymphocytic hypophysitis	2
Neurosarcoidosis	1
Granulomatous angiitis	1
Lymphomatoid granulomatosis	1
Vasculitis	7 (10.4%)
CSF analysis	62 (92%)
Pleocytosis	19 (30.6%)
Increased protein count	27 (43.5%)
FDG PET-CT activity	32 (47.4%)
Increased	18

CSF: Cerebrospinal fluid, FDG: Fluorodeoxyglucose, PET-CT: Positron emission tomography-computed tomography, PML: Progressive multifocal leukoencephalopathy

both), T2W signal intensity, DWI signal with apparent diffusion coefficient (ADC) values, presence or absence of “blooming” on SWI, and enhancement pattern. T2W signal intensity was categorized as homogeneous hyperintense, predominantly intermediate, or heterogeneous (dark mottled areas in a hyperintense background). The ADC values were measured on the workstation by placing the regions of interest in the darkest area of the lesion. Gadolinium enhancement pattern was categorized as absent, micronodular (<3 mm), macronodular (>3 mm), linear, peripheral, and confluent.

RESULTS

Patient profile

Of the 67 patients, 42 were male and 25 were female (ratio: 1.6:1). The median age was 37 years (range: 18–72 years).

Clinical features

Patients presented with a constellation of clinical symptoms, of which hemiparesis (55%, 37/67) and rapid cognitive decline (29.8%, 20/67) were most common. Fever was not exclusive to infections, since five patients diagnosed with lymphoma also presented with a low-grade fever.

Treatment and follow-up

Of the 67 patients who initially received short-course intravenous steroids, 26 were later classified as inflammatory disorders based on clinical or imaging response to steroids [Figure 1]. The remaining 41/67 patients showed clinical or imaging deterioration or steroid unresponsiveness, and 28 of them underwent a stereotactic brain biopsy. A definitive diagnosis of primary B-cell CNS lymphoma was obtained in 20 of these patients ($P = 0.03$). The criteria for imaging deterioration were progression in the extent of parenchymal lesions, development of new lesions [Figure 2], or progression in post-contrast enhancement [Figure 3]. The treatment for this group was subsequently changed to chemoradiotherapy, but 3/20 patients continued to show disease progression despite treatment modification and succumbed to illness within 12 months of treatment initiation.

Of the 13/41 patients that did not undergo biopsy, five were clinically suspected to be lymphoma, but biopsy confirmation could not be obtained as the patients were lost to further follow-up. The remaining (8/13) patients were diagnosed with vasculitis, immune-mediated conditions, PML, and tuberculosis based on positive immune markers or blood cultures.

Neuroimaging

A summary of the baseline MRI features of all the conditions is presented in Table 2. Lymphoma was most commonly seen as multifocal lesions involving both supratentorial and infratentorial parenchyma (19/28, 67.8%), both gray and white matter (20/28, 71%) and in bilaterally symmetric distribution (19/28, 67.5%). The optic nerve pathway, pituitary, and pineal gland were involved in a few cases (9/20). Abnormal spinal cord signal intensity was noted in only 3/17 (17.6%) patients. Macronodular (11/28, 39%) and linear (10/28, 35.7%) were the typical enhancement patterns, while 5 (19.4%) patients showed no post-contrast enhancement. Peripheral and open ring-like enhancement patterns were more commonly associated with inflammatory

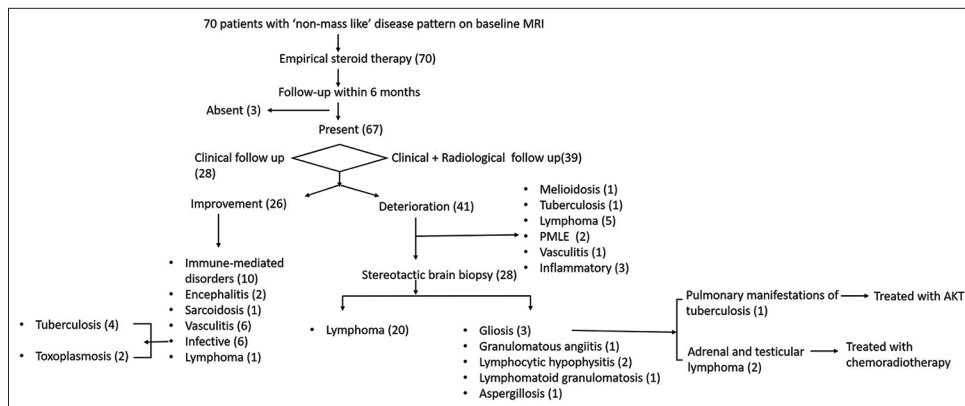


Figure 1: Schematic representation of diagnoses and treatment evolution in patients presenting with non-mass-like infiltrative lesions on MRI brain. AKT: Anti Koch's therapy, PMLE: Progressive multifocal leucoencephalopathy.

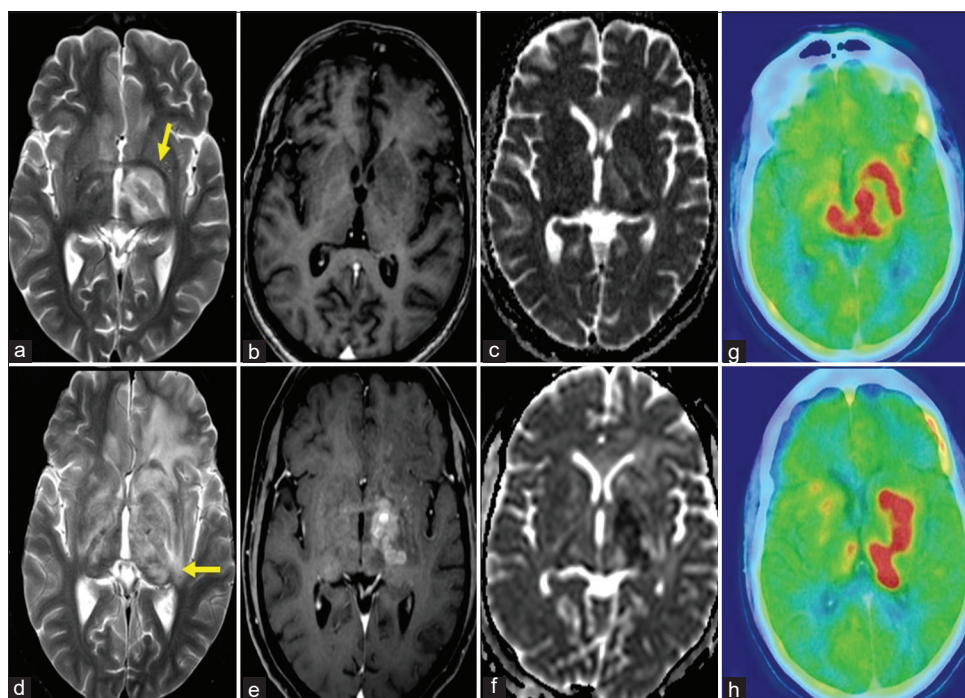


Figure 2: A 34-year-old male with lymphomatosis cerebri. Baseline axial T2W MRI (a) of the brain shows an intermediate to hyperintense lesion in left gray nuclei. There is no contrast enhancement (b), but areas of mild low ADC values are seen (c). Post-treatment MRI brain (d-h) shows disease progression in the form of extensive areas of disease involvement in bilateral deep gray and white matter, along with new areas of nodular and confluent enhancement (e) and low ADC values (f). PET-CT showed new areas of increased radiotracer activity (g and h). ADC: Apparent diffusion coefficient, PET-CT: Positron emission tomography-computed tomography.

conditions. Overall, there was no significant association of lymphoma with regard to lesion location, signal intensity, or enhancement ($P = 0.054$) [Figure 4].

The average ADC values for the lymphoma group were significantly lower ($0.681 \times 103 \text{ mm}^2/\text{s}$) than a mean of $0.803 \times 103 \text{ mm}^2/\text{s}$ combined for other pathologies ($P = 0.007$). The mean difference in ADC value with the adjacent normal brain parenchyma was also found to be higher for lymphomas ($P = 0.03$) [Table 3].

The presence of numerous microhemorrhagic foci on SWI was significantly associated with patients with the final clinical diagnosis of vasculitis (6/7, 85.7%) ($P = 0.002$) [Figure 5].

FDG PET-CT imaging

Whole-body FDG PET-CT showed increased metabolism in the affected areas of the brain in 18/32 (58.1%) patients. Significant association with increased PET-CT activity was

Table 2: Descriptive data of patient findings (percentage in brackets next to numbers) divided into broad categories of lymphoma, inflammatory process, vasculitis, and infective etiologies.

Imaging findings	Diagnosis			
	Number of patients (n=67)			
	Vasculitis 7 (10.4%)	Inflammatory 22 (32%)	Infections 10 (14.9%)	Lymphoma 28 (41.7%)
Location				
Supratentorial (25)	4 (57.1)	7 (31.8)	4 (40)	10 (35.7)
Infratentorial (3)	1 (14.3)	2 (9.1)	-	-
Both (39)	2 (28.6)	13 (59.1)	6 (60)	18 (64.3)
Distribution				
Symmetric (19)	1 (14.3)	10 (45.5)	1 (10)	7 (25)
Asymmetric or unilateral (48)	6 (85.7)	12 (54.5)	9 (90)	21 (75)
Other areas				
Optic nerve pathway (9)	-	3 (13.6)	1 (10)	5 (17.9)
Pituitary gland or stalk (10)	1 (14.3)	5 (22.7)	-	4 (14.3)
Pineal gland (1)	-	-	-	1 (3.6)
Mammillary body (1)	-	1 (4.5)	-	-
T2W signal				
Homogeneously hyperintense (21)	2 (28.6)	8 (36.4)	2 (20)	9 (32.1)
Intermediate-hypointense (46)	5 (71.4)	13 (59.1)	8 (80)	20 (71.4)
Mottled hypointense areas in a hyperintense background (33)	4 (57.1)	11 (50)	6 (60)	12 (42.9)
Contrast enhancement				
Nil (13)	1 (14.3)	6 (27.3)	1 (10)	5 (17.9)
Micronodular (23)	4 (57.1)	7 (31)	5 (50)	7 (25)
Macronodular (24)	3 (42.9)	6 (27.3)	4 (40)	11 (39.2)
Linear or irregular (4)	2 (28.6)	1 (4.5)	1 (10.0)	-
Peripheral incomplete rim (5)	1 (14.3)	3 (13.6)	1 (10.0)	-
Confluent (19)	2 (28.6)	4 (18.2)	2 (20)	11 (39.3)
Diffusion restriction				
Present (35)	1 (14.3)	11 (50)	3 (30)	20 (71.4)
Mean ADC	864	773	788	690
SWI “blooming”				
Present (21)	6 (85.7)	9(40.9)	3 (30)	3 (10.7)
MRI spine (14)				
T2W hyperintense signal	1/5(20)	9/21 (42.9)	1/7 (14.3)	3/20 (15)
Increased FDG PET activity (18)				
Present	2 (50)	3 (33.3)	1 (33.3)	12 (80)

There were no patients showing findings corresponding to the cells marked by “-.” ADC: Apparent diffusion coefficient, SWI: Susceptibility-weighted imaging, FDG: Fluorodeoxyglucose, PET-CT: Positron emission tomography-computed tomography

noted in patients with lymphoma (12/15, 66.7%, $P = 0.017$) with a mean standardized uptake value of 21 [Figure 2]. No pathological extracranial uptake was found.

CSF analysis

CSF profile was available for 62/67 (92%) patients and showed the presence of oligoclonal bands, JC virus antigen, or anti-N-methyl-D-aspartate receptor antigen. These were useful to diagnose non-lymphoma conditions. No atypical cells were found in the CSF, even in the patients with lymphoma. CSF cultures were also non-contributory to any diagnosis. Pleocytosis (30.6%, 19/62) or elevated CSF protein levels (40%, 27/62) also did not favor any particular diagnosis.

Systemic manifestations

Systemic disease manifestations (intrapulmonary cavities and enlarged mediastinal nodes), blood serology, and response to antitubercular therapy enabled the diagnosis of tuberculosis in five patients. Ankle joint septic arthritis and positive joint aspirate culture results led to the diagnosis of melioidosis in one instance. Fungal elements in blood culture contributed to the diagnosis of aspergillosis in one patient [Figure 6]. Serum toxoplasmosis-IgG was positive in two immunocompromised patients diagnosed with toxoplasmosis. Serum angiotensin-converting enzyme level was elevated in one patient diagnosed with sarcoidosis.

DISCUSSION

Diffusely infiltrative “non-mass-like” brain parenchymal abnormalities with minimal to absent contrast enhancement

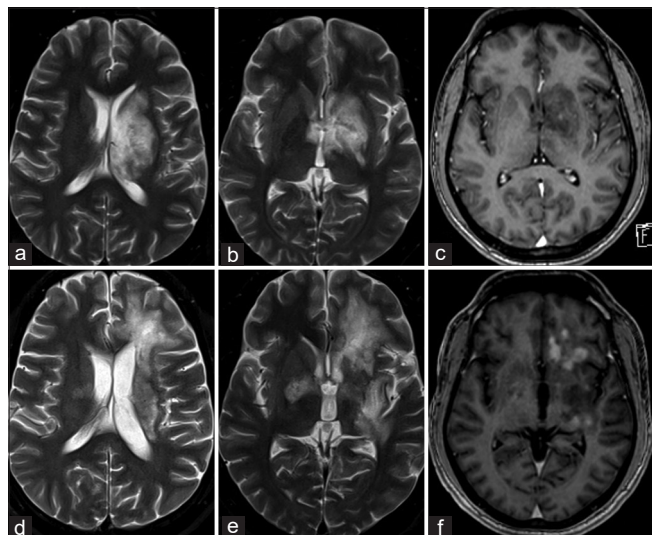


Figure 3: A 40-year-old male with lymphomatosis cerebri. Baseline axial T2W MRI (a and b) shows a predominantly T2W hyperintense lesion with interspersed intermediate signal areas, in the left periventricular white matter and basal ganglia. A small focus of micronodular contrast enhancement is seen within (c). Follow-up MRI brain (d-f) after 4 months of steroid therapy shows an increase in the extent of the lesion in bilateral cerebral parenchyma. New areas of macronodular contrast enhancement also suggest disease progression (f).

and variable ADC values can be seen in a host of benign and malignant conditions. The benign spectrum is more common and typically includes immune-mediated or demyelinating conditions, sarcoidosis, and small-vessel vasculitis,^[5,6] whereas the malignant end of this spectrum comprises an unusual variety of non-Hodgkin’s lymphoma, termed “LC.”^[3] To date, only a few isolated case reports describing imaging features in LC have appeared in the literature.^[7] Its rarity and lack of specific imaging findings can lead to misdiagnosis.^[8] Since the majority of the conditions typically have a benign course and respond to empirical steroids, patients are kept on observation with follow-up at intervals. This may lead to delayed diagnosis of LC. Although lymphomatosis is generally fatal,^[3,9] literature reports clinical improvement and even remission after combination chemoradiotherapy if diagnosed early.^[10]

We present our experience of 67 cases presenting “non-mass” parenchymal abnormality on MRI brain. Almost all our patients were initially thought to represent diffuse leukoencephalopathy secondary to immune-mediated or inflammatory processes and were started on oral or intravenous steroids. We broadly classified the conditions into lymphoma and non-lymphoma, based on their eventual diagnoses in an attempt to identify imaging features that help differentiate lymphoma from other conditions.

The clinical spectrum was dominated by altered cognitive status and focal neurological deficits. Similar to prior case reports, progressive cognitive decline was commonly noted in patients with lymphomatosis, despite steroid therapy.^[2,7]

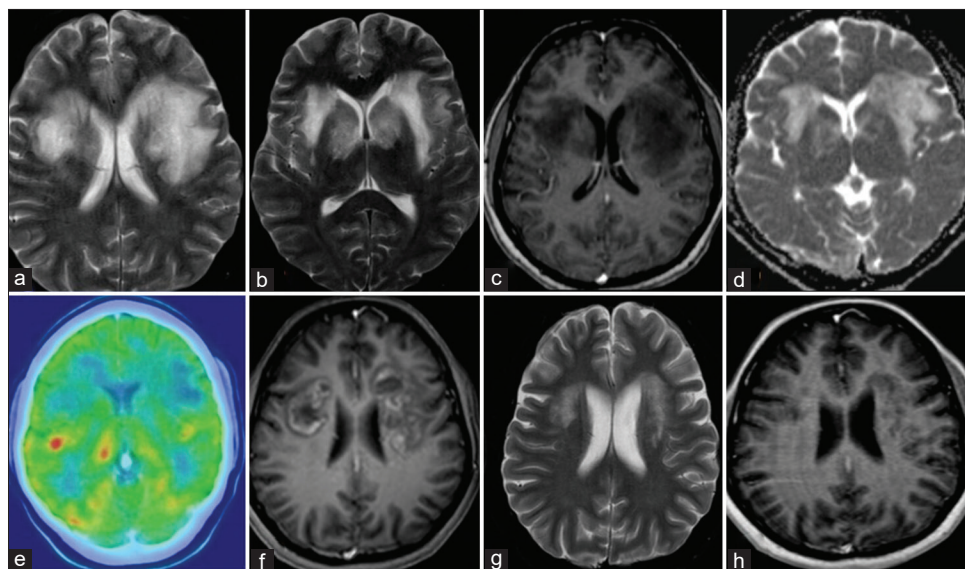


Figure 4: A 45-year-old female with immune mediate disease. Baseline axial T2W MRI (a and b) shows T2W hyperintense lesion involving bilateral corona radiata in a symmetrical distribution. There is no contrast enhancement (c) or low signal on ADC (d). PET-CT imaging does not show increased activity in the areas of interest (e). Subsequent follow-up MRI brain done 3 months later shows new development of peripheral incomplete rim-like areas of enhancement (f). Steroid therapy was continued and there was significant disease regression followed by the disappearance of enhancement, another 6 months later (g and h). ADC: Apparent diffusion coefficient, PET-CT: Positron emission tomography-computed tomography.

Table 3: Comparison of potential diagnostic variables on imaging to differentiate between lymphoma and mimicking conditions. Diffusion restriction with low ADC values, higher drop in ADC values in the lesion compared to normal parenchyma (mean ADC difference), and increased FDG PET-CT activity are important clues to diagnose lymphomatosis.

	Lymphoma (26)	Non-lymphomas (38)	P-value
MRI findings			
Location			
Supratentorial	10 (38.3%)	15 (38.5%)	0.288
Infratentorial	-	3 (7.7%)	
Both	18(64.3%)	21 (53.8%)	
Gray matter	2 (7.1%)	-	0.047
White matter	5 (17.9%)	15 (41.7%)	
Both	21 (75%)	21 (58.3%)	
Distribution			
Bilateral asymmetric or unilateral	21 (75%)	7 (69.2%)	0.605
Symmetric	7 (25%)	12 (30.8%)	
T2W signal			
Homogeneously hyperintense	9 (32.1%)	12 (30.8%)	0.905
Intermediate to hypointense	20 (71.4%)	26 (66.7%)	0.679
Mottled hypointense areas in hyperintense background	12 (42.9%)	21 (53.8%)	0.375
Contrast enhancement			
Nil	5 (17.9%)	8 (20.5%)	0.786
Micronodular (<3 mm)	7 (25%)	16 (41%)	0.173
Macronodular (>3 mm)	11 (35.9%)	13 (46.4%)	0.386
Peripheral incomplete rim	-	5(12.8%)	0.049
Linear or irregular	-	4 (10.3%)	0.081
Amorphous cloud-like or confluent	11 (39.3%)	8 (20.5%)	0.093
Diffusion restriction			
Present	20 (71.4%)	15 (38.5%)	
Mean ADC (lesion)	690.6	806.7	0.007
Mean ADC difference (lesion – normal ([780])	90.4	-8.3	0.03
SWI “blooming”			
Present	3 (10.7%)	8 (46.2%)	0.002
FDG PET-CT			
Activity present	12/15 (80%)	6/16 (37.5%)	0.017
Disease progression			
Present	27 (96.4%)	14 (35.9%)	0.00

ADC: Apparent diffusion coefficient, SWI: Susceptibility-weighted imaging, FDG: Fluorodeoxyglucose, PET-CT: Positron emission tomography-computed tomography

Elevated serological marker levels such as oligoclonal IgG bands and antinuclear antibodies were found in immune-mediated disorders and vasculitis. Although autoantibodies are quite specific, their absence cannot rule out autoimmune conditions, as in 80% (53/67) of our cases, laboratory and immune workup results were non-contributory. Nonetheless, serological markers should be included in the routine workup, as they do help narrow the differentials, if positive.

Studies have shown that lesion location can provide clues to differentiate lymphoma from other conditions. For instance, lymphoma has been reported to have a higher tendency to bilaterally involve the deep periventricular white matter, as compared to immune-mediated conditions that tend to be unilateral and more peripherally located. Sato *et al.*^[11] and Li *et al.*^[12] suggested that spinal cord involvement should

increase the suspicion for lymphomatosis. However, in our patient group, the location was not a significant factor in differentiating between lymphoma and non-lymphoma groups.

On MRI imaging, diffusion restriction with low ADC values was found to be the one potentially useful feature favoring lymphoma. Although this finding is already established as a key factor in distinguishing between mass-like lymphomas and other primary brain neoplasms, there is no conclusive evidence regarding its reliability in identifying the infiltrative variety of lymphoma. Yu *et al.* reported the presence of facilitated diffusion in a series of seven cases of LC,^[13] whereas Izquierdo *et al.* found a diffusion restriction pattern in 66.7% (6/9) patients.^[9] Another case report by Li *et al.* showed the presence of areas of both T2W shine-through effect as well as

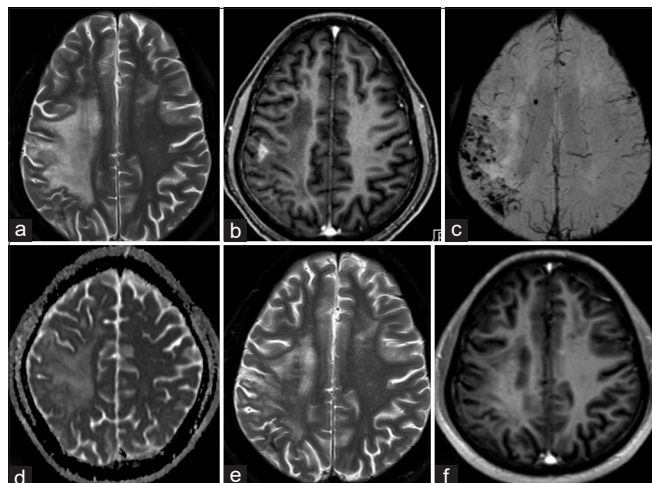


Figure 5: A 32-year-old female with vasculitis. Baseline axial T2W MRI (a) shows an ill-defined hyperintense lesion in the right centrum semi-ovale, with a single focus of macronodular enhancement (b). Numerous microhemorrhages showing “blooming” are noted on SWI (c). Follow-up MRI brain (d-f) after 5 months of steroid therapy showed a significant interval decrease in the T2W hyperintense areas and resolution of the enhancement. SWI: Susceptibility-weighted imaging.

slight restricted diffusion within the lesions.^[12] Overall, the diagnostic value of DWI should not be undermined as the variation in DWI signal and ADC values may be a result of regional variations in tumor cellular density.

The presence of disease activity on PET-CT was also found to be valuable to raise a suspicion of lymphoma. In contrast, Kawai *et al.* compared the FDG PET activity in 12 patients with typical and five patients with atypical MRI features of lymphoma and concluded that the value of PET-CT appears to be limited in differentiating atypical lymphoma from other diseases.^[14] Similarly, Chen and Dong also found low FDG uptake in non-enhancing CNS lymphomas.^[15] The conflicting results could be due to steroid administration before the PET-CT.

Because of the initial diagnostic dilemma, a trial of steroids can be offered to alleviate the clinical symptoms. However, initial improvement with steroids should be interpreted with caution. Studies have shown that therapy with high-dose steroids in patients with LC can induce a transient clinical and in some instances, a radiological response as well. An eventual clinical deterioration is, however, inevitable. Steroids also contribute to false-negative biopsies delaying

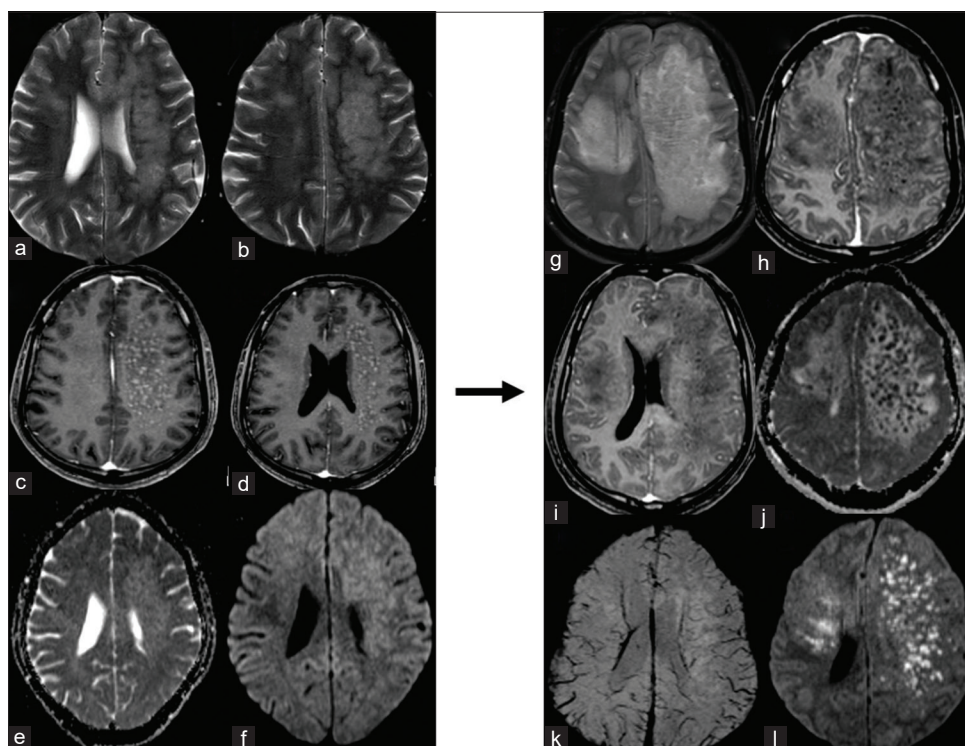


Figure 6: A 40-year-old male with aspergillosis infection. Baseline (a-f) and post-steroid therapy MRI brain (g-l) show T2W intermediate signal area with hypointense nodular areas within, in the left cerebral white matter (a and b). Numerous micronodular enhancing foci (c and d) and areas of mildly low ADC values (e and f) were also noted. Following steroid administration, the disease progressed with a more aggressive appearance spreading to contralateral parenchyma (g-i). Multiple new areas of low ADC also appeared (j and l). Fungal elements were found in the blood culture. ADC: Apparent diffusion coefficient

the definitive diagnosis for months.^[16] This may explain the initial inconclusive histopathology results in two of our patients who eventually showed systemic evidence of lymphoma outside the neuraxis later in the course of the disease. For this reason, until the diagnosis is established, steroids should ideally not be prescribed if there is a suspicion of lymphoma except in cases of severe clinical deterioration in which case, steroid therapy can be potentially lifesaving. Stereotactic tissue biopsy remains the gold standard.^[10] Rapid clinical deterioration, presence of diffusion restriction in extensive infiltrating brain lesions, increased PET activity, and non-response to steroid trial should raise the alarm bells for lymphoma, and early biopsy should be recommended instead of continuing immunosuppressive therapies which are ineffective in the long run. Positivity for serological markers of immune-mediated or inflammatory disorders, systemic manifestations of infections, parenchymal microhemorrhages, or peripheral open-ring enhancement supports alternate diagnoses.

Besides traditional MRI, perfusion MRI and MR spectroscopy (MRS) are well-established methods to differentiate CNS lymphomas from their benign mimickers.^[17] On MR perfusion, relative cerebral blood volume (rCBV) is increased in lymphoma but reduced in inflammatory or immune-mediated conditions. On MRS, elevated lipid peaks combined with high choline/creatine and choline/NAA ratios can provide clues to the diagnosis of lymphoma.^[4] However, there is limited literature with inconsistent results evaluating the value of these advanced imaging techniques to differentiate lymphomatosis from mimics. Studies have reported both high and normal choline/NAA ratios on MRS for lymphomatosis.^[2,12,17] Similarly, rCBV may or may not be elevated on perfusion MRI due to the variable permeability of the blood–brain barrier.^[9,13,18]

Limitations

Histopathology was not available for 41 patients who were treated based on a presumptive diagnosis. The diagnostic value of MRI perfusion and spectroscopy was not assessed due to non-uniformity in the institutional imaging protocol and processing software used for our cases. In addition, these advanced sequences were not available for all patients. We did not assess long-term survival and prognosis for our study group due to insufficient data. MRI spine results in this study may be under-representative of spinal cord involvement, as spine imaging was only performed for symptomatic cases.

CONCLUSION

The discrimination between LC and its less aggressive mimics can be attempted with DWI-MRI and FDG PET-CT when read in conjunction with rapid progression of clinical

features, serological workup, and systemic evaluation. We emphasize the importance of alerting the clinicians about LC early so that prompt early biopsy is performed, and the appropriate therapy can be initiated.

Declaration of patient consent

Institutional Review Board (IRB) permission obtained for the study.

Financial support and sponsorship

Nil.

Conflicts of interest

There are no conflicts of interest.

REFERENCES

1. Leclercq D, Trunet S, Bertrand A, Galanaud D, Lehericy S, Dormont D, *et al.* Cerebral tumor or pseudotumor? *Diagn Interv Imaging* 2014;95:906-16.
2. Murakami T, Yoshida K, Segawa M, Yoshihara A, Hoshi A, Nakamura K, *et al.* A case of lymphomatosis cerebri mimicking inflammatory diseases. *BMC Neurol* 2016;16:128.
3. Lee PJ, Berrios I, Ionete C, Smith T. Lymphomatosis cerebri: Diagnostic challenges and review of the literature. *BMJ Case Rep* 2016;2016:bcr2016216591.
4. Courtois F, Gille M, Haven F, Hantson P. Lymphomatosis cerebri presenting as a recurrent leukoencephalopathy. *Case Rep Neurol* 2012;4:181-6.
5. Sarbu N, Shih RY, Jones RV, Horkayne-Szakaly I, Oleaga L, Smirniotopoulos JG. White matter diseases with radiologic-pathologic correlation. *Radiographics* 2016;36:1426-47.
6. Aliaga ES. Vasculitis and Other Inflammatory Disorders. In: *Clinical Neuroradiology*. Berlin: Springer; 2019. p. 809-48.
7. Kerbauy MN, Pasqualin DDC, Smid J, Iquizli R, Kerbauy LN, Nitrini R, *et al.* Diffuse large B-cell lymphoma of the central nervous system presenting as “lymphomatosis cerebri” and dementia in elderly man: Case report and review of the literature. *Medicine (Baltimore)* 2019;98:e14367.
8. Hatanpaa KJ, Fuda F, Koduru P, Young K, Lega B, Chen W. Lymphomatosis cerebri: A diagnostic challenge. *JAMA Neurol* 2015;72:1066-7.
9. Izquierdo C, Velasco R, Vidal N, Sánchez JJ, Argyriou AA, Besora S, *et al.* Lymphomatosis cerebri: A rare form of primary central nervous system lymphoma. Analysis of 7 cases and systematic review of the literature. *Neuro Oncol* 2016;18:707-15.
10. Thurnher MM, Rieger A, Kleibl-Popov C, Settinek U, Henk C, Haberler C, *et al.* Primary central nervous system lymphoma in AIDS: A wider spectrum of CT and MRI findings. *Neuroradiology* 2001;43:29-35.
11. Sato H, Takahashi Y, Wada M, Shiono Y, Suzuki I, Kohno K, *et al.* Lymphomatosis cerebri with intramedullary spinal cord involvement. *Intern Med* 2013;52:2561-5.
12. Li L, Rong JH, Feng J. Neuroradiological features of

- lymphomatosis cerebri: A systematic review of the English literature with a new case report. *Oncol Lett* 2018;16:1463-74.
13. Yu H, Gao B, Liu J, Yu YC, Shiroishi MS, Huang MM, *et al.* Lymphomatosis cerebri: A rare variant of primary central nervous system lymphoma and MR imaging features. *Cancer Imaging* 2017;17:26.
 14. Kawai N, Okubo S, Miyake K, Maeda Y, Yamamoto Y, Nishiyama Y, *et al.* Use of PET in the diagnosis of primary CNS lymphoma in patients with atypical MR findings. *Ann Nucl Med* 2010;24:335-43.
 15. Chen H, Dong H. A rare case of nonenhancing primary central nervous system lymphoma mimic multiple sclerosis. *Neurosciences (Riyadh)* 2015;20:380-4.
 16. Rollins KE, Kleinschmidt-Demasters BK, Corboy JR, Damek DM, Filley CM. Lymphomatosis cerebri as a cause of white matter dementia. *Hum Pathol* 2005;36:282-90.
 17. Haldorsen IS, Espeland A, Larsson EM. Central nervous system lymphoma: Characteristic findings on traditional and advanced imaging. *AJNR Am J Neuroradiol* 2011;32:984-92.
 18. da Rocha AJ, Guedes BV, da Silveira da Rocha TM, Maia AC Jr., Chiattoni CS. Modern techniques of magnetic resonance in the evaluation of primary central nervous system lymphoma: Contributions to the diagnosis and differential diagnosis. *Rev Bras Hematol Hemoter* 2016;38:44-54.

How to cite this article: Patra A, Jasper A, Vanjare H, Chacko G, Susheel S, Sivadasan A, *et al.* Diffuse infiltrative non-mass-like brain parenchymal lesions on MRI: Differentiating lymphomatosis cerebri from its mimics. *J Clin Imaging Sci* 2021;11:41.